BMC Biology

RESEARCH

Open Access

Identification and functional characterization of AsWRKY9, a WRKY transcription factor modulating alliin biosynthesis in garlic (*Allium sativum* L.)

Jiaying Wu[1†], Min Li[1†], Wanni Wang[1], Yiren Su[1], Jie Li[1], Jiaxin Gong[1], Xianfeng Meng[2], Chenyuan Lin[1], Qiantong Zhang[1], Yanyan Yang[2], Chunyan Xu[1], Limei Zeng[1], Jihong Jiang[1*] and Xuqin Yang[1*]

Abstract

Background The variations in alliin content are a crucial criterion for evaluating garlic quality and is the sole precursor for allicin biosynthesis, which is significant for the growth, development, and stress response of garlic. WRKY transcription factors are essential for enhancing stress resistance by regulating the synthesis of plant secondary metabolites. However, the molecular mechanisms regulating alliin biosynthesis remain unexplored. Here, we report for the first time that a WRKY family transcription factor regulates the expression of a key enzyme gene in the alliin biosynthesis pathway, enhancing the accumulation of alliin.

Results AsWRKY9 was most highly expressed in garlic leaves, and its expression was significantly upregulated at various time points following leaf injury. Moreover, we established an improved garlic callus induction medium based on MS medium with 1.5 mg/L 2,4-D and 0.5 mg/L NAA, suitable for "PiZi" garlic bulbils. In transgenic callus overexpressing AsWRKY9, the transcription level of the key enzyme flavin-containing monooxygenase gene (*AsFMO1*) significantly higher, as did its enzymatic activity compared with the control. Subcellular localization revealed that AsWRKY9 is located in the nucleus. The promoter sequence of *AsFMO1* was then obtained using genomee walking. Yeast one-hybrid (Y1H) and dual-luciferase assays (LUC) confirmed that AsWRKY9 interact with the *AsFMO1* promoter. Further verification by electrophoretic mobility shift assay (EMSA) and chromatin immunoprecipitation qPCR (ChIP-qPCR) confirmed that AsWRKY9 interacts by binding to the W-box site on the *AsFMO1* promoter. Compared to the control, the alliin content in the transgenic callus overexpressing AsWRKY9 was significantly increased, thus confirming the activation of the alliin biosynthesis pathway and enhancing the accumulation of alliin in garlic.

Conclusions Our study reveals the crucial role of AsWRKY9 in alliin biosynthesis, filling a gap in the complex transcriptional regulation of the alliin biosynthetic pathway. It provides a new molecular breeding strategy for developing garlic varieties with high alliin content.

Keywords Transcription factor, WRKY, Garlic, *AsFMO1*, Alliin biosynthesis

†Jiaying Wu and Min Li contributed equally to this work.

*Correspondence:
Jihong Jiang
jhjiang@jsnu.edu.cn
Xuqin Yang
xuqinyang@jsnu.edu.cn
Full list of author information is available at the end of the article

Background

Garlic (*Allium sativum* L., 2n = 2x = 16), a member of the *Allium* genus within the *Amaryllidaceae* family, has been widely cultivated worldwide for over 5000 years [1, 2] and is valued as a vegetable, medicinal plant, and a spice [3, 4]. Both the leaves and bulbs of garlic are rich in essential trace elements such as selenium, manganese, zinc, iron, and vitamins, as well as polysaccharides and sulfides, conferring significant medicinal and economic value [5, 6]. The distinctive pungent flavor and medicinal properties of garlic are primarily attributed to allicin, a volatile organic sulfur compound [7]. Allicin content as a core quality metric for garlic. Allicin has been proven to possess potent antibacterial [8], anti-inflammatory [9], anticancer [10], immune-enhancing [11], and cardiovascular disease-treating [12] properties. Interestingly, allicin is not inherently present in garlic but is produced through an enzymatic reaction when garlic cells are crushed, combining alliinase in the vacuoles with its precursor alliin in the cytoplasm [13]. However, the yield of allicin obtained from natural garlic through traditional methods remains exceedingly low, insufficient to meet the increasing market demand.

Alliin, the sole precursor in the allicin biosynthetic pathway, plays a critical role in this process [14]. Promoting alliin biosynthesis in garlic through molecular biology techniques represents the most direct and effective method to enhance allicin content. Research has identified that the primary site of alliin biosynthesis is in mature leaf tissue [15]. Notably, when new leaves develop, the stored alliin in mature leaves is transported to the young leaves, thus protecting the sprouts from microbial and herbivorous threats [14]. This mechanism reflects an evolutionary self-protection strategy developed by garlic. Currently, the alliin biosynthetic pathway in garlic remains poorly understood. Based on radiotracing experiments and chemical analyses, the proposed biosynthetic pathway [16–19] includes the initial combination of cysteine and glutamate, followed by the coupling of glycine with γ-glutamylcysteine, then the S-conjugation of glutathione, removal of the glycine moiety, modification of the S-alk(en)yl group, removal of the γ-glutamyl group, and finally S-oxidation. It has been confirmed that γ-glutamyl transpeptidase genes (*AsGGT1*, *AsGGT2*, and *AsGGT3*) and a flavin-containing monooxygenase gene (*AsFMO1*) catalyze the final two steps of this pathway, converting basic amino acids into biologically active alliin. Current studies on alliin biosynthesis in garlic remain limited. Sun et al. [20] sequencing, assembly, and analysis of the garlic genome suggested that four *GSH1* homologous genes, one *GSH2* homologous gene, and one *PCS* homologous gene are potential candidates for future research on alliin biosynthesis.

Transcription factors (TFs) are multifunctional proteins that play a crucial role in many signaling pathways [21]. WRKY TFs, one of the largest families of plant transcription factors [22], are classified into 3 groups (I, II, III) based on the number of WRKY domains and the characteristics of the zinc finger domains [23]. They play crucial roles in plant responses to biotic and abiotic stresses [24], growth and development [25], and secondary metabolism [26]. Xiao et al. discovered that GhWRKY41 forms a positive feedback loop, enhancing lignin and flavonoid to resist infection by *Verticillium dahliae* in cotton [27]. Tao et al. proposed that, when plants in the *Brassicaceae* family are infected with *Alternaria brassicicola*, WRKY33 induces the expression of MYB51 and CYP83B1, promoting the biosynthesis of the precursor indole glucosinolate (I3G) to 4-methoxyindol-3-ylmethyl glucosinolate (4MI3G), which exerts a protective effect [28]. Yuan et al. found that SlWRKY35 directly binds to the promoter of SlDXS1 in tomatoes, significantly upregulating the expression of methylerythritol phosphate (MEP) pathway genes and increasing the content of downstream metabolites [29]. An increasing number of WRKY transcription factors have been identified as key regulators in plant metabolism. However, reports on the molecular regulation of alliin biosynthesis in garlic remain limited. Through transcriptomic analysis, Yang et al. speculated that 8 TFs, including MYB, AP2/ERF, and NAC families, may be involved in regulating alliin biosynthesis [30], with no functional studies on WRKY TFs in regulating alliin biosynthesis in garlic reported to date.

In this study, based on the previous garlic transcriptome database [30], 21 WRKY genes were identified. Gene expression levels in garlic crushed leaves and overexpressed callus were analyzed using quantitative real-time PCR (qRT-PCR), which identified AsWRKY9 as a candidate gene regulating alliin biosynthesis. Subcellular localization, Y1H, EMSA, LUC, and ChIP-qPCR analyses confirmed that AsWRKY9 binds to the W-box region of the promoter of the key oxidase *AsFMO1* in the alliin biosynthesis pathway, positively enhancing *AsFMO1* expression and promoting alliin accumulation in garlic. This study is the first to propose a transcription factor, AsWRKY9, positively regulating the biosynthesis of alliin, filling a gap in the molecular regulation of the alliin biosynthesis pathway, expanding our understanding of alliin biosynthesis, and providing potential genetic resources for breeding garlic varieties with high alliin content.

Results

Callus tissue culture and genetic transformation

Research detailed in Additional file 1: Table. S1 reveals a notable dependency between the rates of callus induction in "PiZi" garlic and the concentrations of 2,4-D and

NAA used. Higher concentrations of 2,4-D and NAA resulted in a decrease in callus induction rates, with only a 20% success rate observed. In contrast, optimal results-achieving an 80% induction rate-were obtained with 1.5 mg/L 2,4-D and 0.5 mg/L NAA. When the NAA concentrations was increased beyond level, induction rates dropped below 40%. The most effective hormonal regimen for inducing callus tissue in "PiZi" garlic bulbs was found to be MS basal medium supplemented with 1.5 mg/L 2,4-D and 0.5 mg/L NAA. We have optimized the transformation system, increasing the genetic transformation efficiency of garlic callus to 20%.

Identification and confirmation of AsWRKY9 as a key candidate gene

From the heatmap, it can be observed that at 3 h of clamping treatment, the expression levels of *AsWRKY3*, *AsWRKY4*, *AsWRKY9*, *AsWRKY19*, and *AsWRKY21* were significantly upregulated, increasing by 2.50- to 5.59-fold compared with the control. At 6 h of treatment, the expression levels of all genes were lower than the control, except for *AsWRKY9*, which remained significantly upregulated with a 1.64-fold increase. At 12 h of treatment, the expression levels of *AsWRKY3*, *AsWRKY4*, *AsWRKY9*, and *AsWRKY19* showed the most significant increases. Overall, the analysis indicates that *AsWRKY9* remained consistently upregulated at different time points, followed by *AsWRKY3*, *AsWRKY4*, *AsWRKY19*, and *AsWRKY21*, which also exhibited higher expression levels (Fig. 1A).

Domain predictions analysis for AsWRKY3, AsWRKY4, AsWRKY9, AsWRKY19, and AsWRKY21 revealed that all of them contain a WRKY domain. Additionally, AsWRKY9 has a Plant-zn-clust domain, suggesting a potentially distinct function compared to other genes (Fig. 1B).

Subsequent qRT-PCR analysis was conducted to assess the expression levels of *AsGGT1*, *AsGGT2*, *AsGGT3*, and *AsFMO1* in AsWRKY3-OE, AsWRKY4-OE, AsWRKY9-OE, AsWRKY19-OE, and AsWRKY21-OE. Compared to the control (35S::GFP), AsWRKY4-OE, AsWRKY19-OE, and AsWRKY21-OE significantly increased the expression of *AsGGT1*, while *AsGGT3* was significantly upregulated in AsWRKY4-OE. *AsFMO1* was upregulated in AsWRKY4-OE, AsWRKY9-OE, AsWRKY19-OE, and AsWRKY21-OE, with the most significant increase observed in AsWRKY9-OE (16.2-fold). Based on these results, we hypothesize that AsWRKY9 may participate in the alliin biosynthetic pathway by regulating the expression of *AsFMO1* (Fig. 1C).

Cloning and sequence analysis of AsWRKY9

The *AsWRKY9* gene contained a 804-bp open reading frame (ORF) that encoded a predicted polypeptide of 267 amino acids with a predicted molecular weight (MW) of

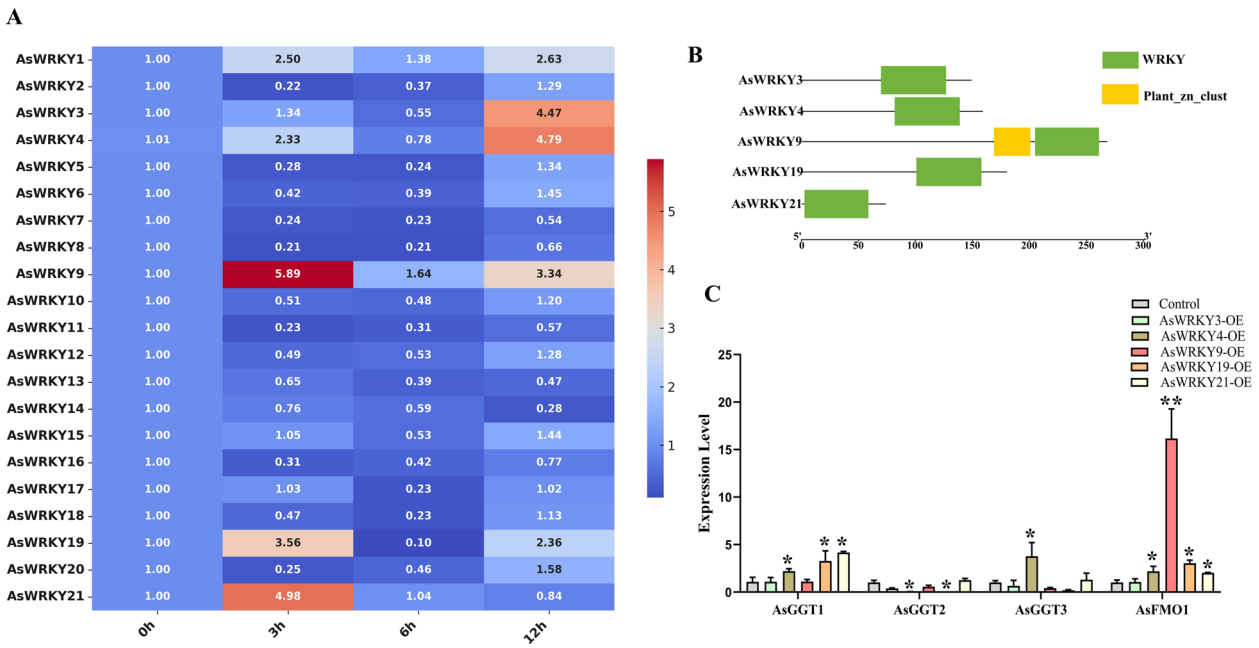

Fig. 1 Characterization of AsWRKYs. **A** Heatmap representation of the expression of *AsWRKY* genes in garlic leaves under clamping treatment (0 h, 3 h, 6 h, or 12 h). **B** Conserved domains in predicted AsWRKY protein sequences. **C** The qRT-PCR analysis of the expression of alliin biosynthesis-related genes in the control (35S:GFP-OE) and in the AsWRKY-OE callus. *AsGAPDH* was set as a reference gene. The *p*-values were evaluated using Student's *t*-test. Stars indicate the level of significance, $^{**}p < 0.01$, and $^{*}0.01 < p < 0.05$

24.5 kDa and an isoelectric point (pI) of 7.95. This protein contains a highly conserved WRKYGQK domain and a C_2H_2 zinc finger motif, classifying it into Group II-d of the WRKY family. Notably, AsWRKY9 shares high sequence identity with proteins from various species, including *Narcissus hybrid cultivar* (NtWRKYY2 AR076402.1 and NtWRKYJ2 AR076403.1, 63.77%), *Iris laevigata* (IlWRKY11 WCL15236.1, 60.29%), *Elaeis guineensis* (EgWRKY51 XP_010929316.1, 59.33%), and *Lilium regale* (LrWRKY16 QRX38913.1, 53.62%) (Fig. 2A). Phylogenetic analysis reveals that AsWRKY9 is closely related to the corresponding protein in *Narcissus hybrid cultivar* (Fig. 2B). Upon comparing with the model organism *Arabidopsis thaliana*, it has been determined that AsWRKY9 shares a high degree of homology with AtWRKY11 (At4G31550.2), classifying both within the subfamily II-d of the WRKY transcription factors (Additional file 2: Fig. S1).

Expression of AsWRKY9 in *Allium sativum* and localization in the nucleus

To investigate the potential working site of AsWRKY9 in *Allium sativum,* we analyzed its expression levels in different tissues, including root, stalk, leaves and bulb. The results revealed that the *AsWRKY9* gene exhibited a high expression level in the leaves (Fig. 2C). The AsWRKY9-GFP fusion protein was transiently expressed in the epidermal cells of *Nicotiana benthamiana* for the purpose of assessing the subcellular localization of AsWRKY9. Confocal microscopy analysis of the GFP fluorescence signal indicated that AsWRKY9 is localized to the nucleus (Fig. 2D).

AsWRKY9 directly binds to the W-box in the *AsFMO1* promoter

To investigate the regulatory role of AsWRKY9 in alliin biosynthesis, we used genome walking to analyze the promoter sequences of *AsFMO1*, identifying a putative W-box motif at −701 to −706 bp. Y1H confirmed direct binding of AsWRKY9 to the AsFMO1-F3 fragment, which contains the W-box. Control experiments with mutated W-box (mAsFMO1) and empty vectors further validated that binding was specific to this site. Only yeast cells co-expressing pB42AD-AsWRKY9 and p178-AsFMO1 turned blue on selective media (Fig. 3). Based on the results from Y1H, AsWRKY9 is likely to bind to the W-box region of *AsFMO1*. To further confirm this interaction, we collected AsWRKY9-OE callus for ChIP-qPCR analysis. The schematic representation

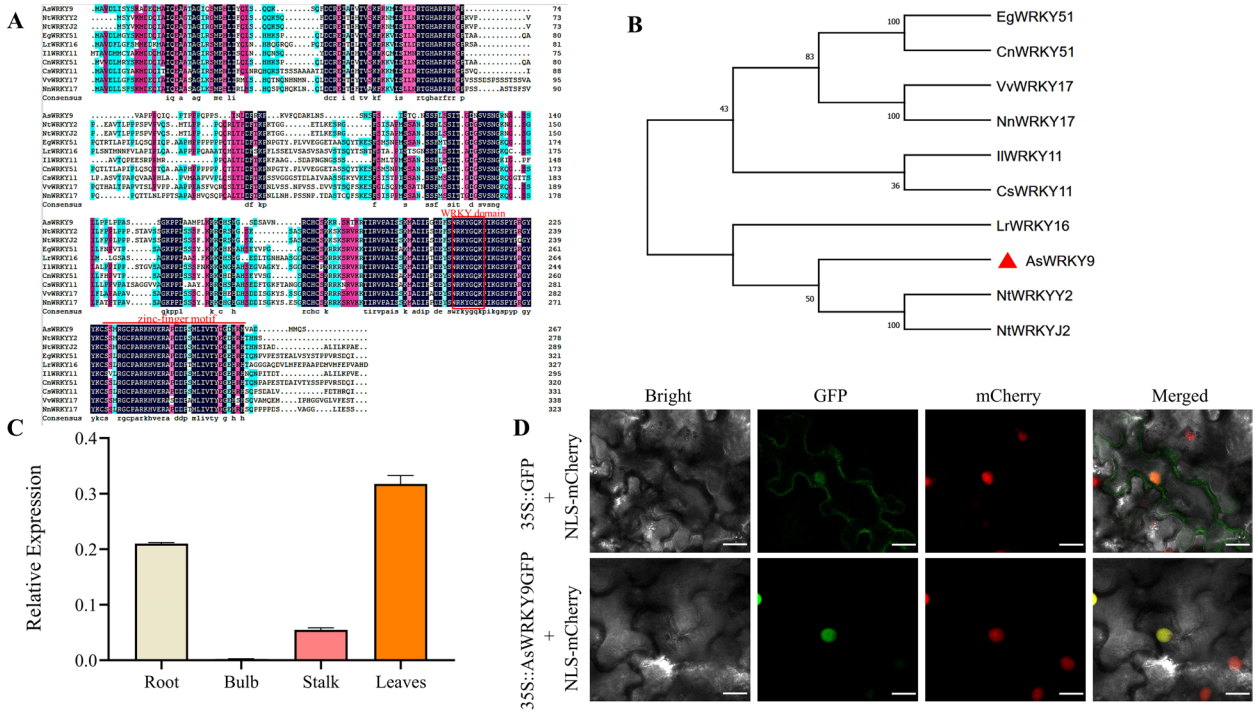

Fig. 2 Sequence analysis, tissue expression pattern analysis, and subcellular localization of AsWRKY9. **A** Protein sequence alignment of AsWRKY9 and its closest homologs from different plant species. The WRKY domain and zinc-finger motif are represented with red lines. **B** Phylogenetic tree of AsWRKY9 with its homologs from the selected plant species. **C** The expression patterns of AsWRKY9 in root, leaves, stalk, and bulb tissues of *Allium sativum* L. **D** Subcellular localization of AsWRKY9 *N. benthamiana* leaves epidermal cells were transformed with the fusion construct (AsWRKY9-GFP) and the nuclear marker NLS-mCherry. Bars = 20 μm

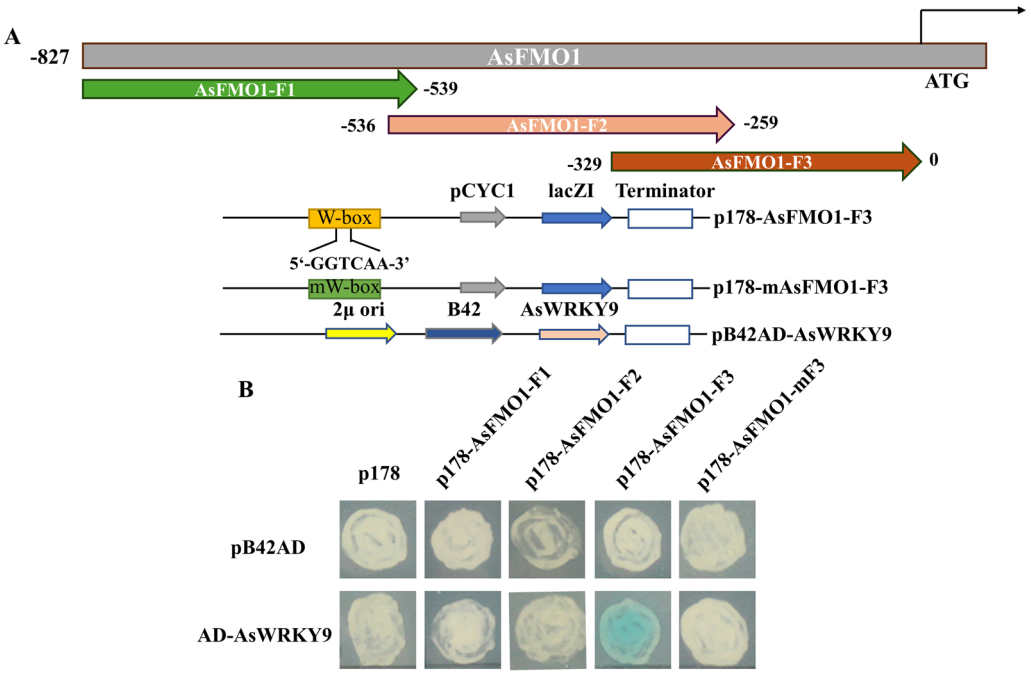

Fig. 3 AsWRKY9 could bind with W-box in yeast. **A** The schematic diagram of the promoter segmentation of *AsFMO1* genes and sketch map of the prey vector and bait vectors. **B** The binding capability tests of AsWRKY9 and *AsFMO1* in yeast by using X-gal. The p178 empty vector and pB42AD/pB42AD-AsWRKY9 were cotransformed into the EGY48 as the control

of the *AsFMO1* promoter region is illustrated in Fig. 4A. As shown in Fig. 4B, the W-box of *AsFMO1* promoter was 6.9-fold enriched than the CDS region of *AsFMO1*, strongly suggesting that AsWRKY9 specifically binds to the *AsFMO1* promoter region.

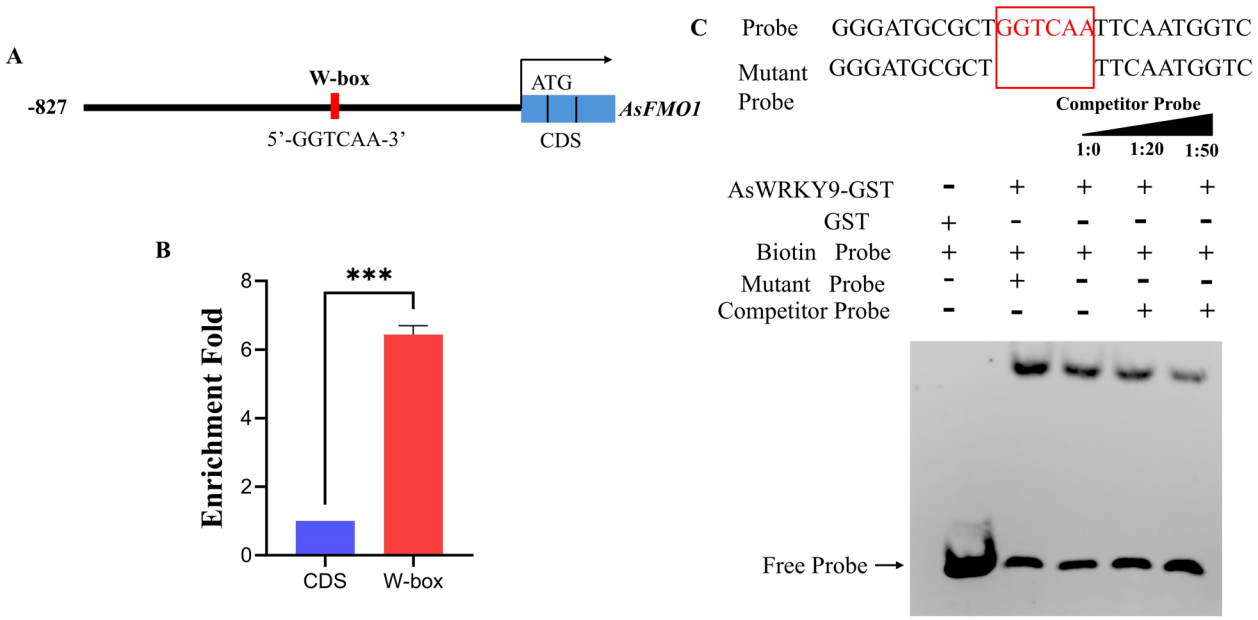

Fig. 4 ChIP-qPCR and EMSA analysis. **A** Schematic representation of the AsFMO1 promoter region and its key regulatory element. The W-box motif is highlighted in red. The CDS of AsFMO1 is indicated in blue. **B** ChIP-qPCR analysis demonstrating the specific enrichment of the W-box region compared to the CDS region. Error bass represent SD for three independent experiments. **C** EMSA showing the interaction between AsWRKY9 and the AsFMO1 promoter. The free probe is indicated at the bottom of the gel. The competitor probe sequences were the same as the labeled probes but without biotin labeling

Finally, to further confirm the direct binding site, EMSA was performed, demonstrating that AsWRKY9 can indeed bind to the W-box motif within the *AsFMO1* promoter in vitro (Fig. 4C). Collectively, both in vivo and in vitro results consistently support the conclusion that AsWRKY9 directly interacts with the W-box of the *AsFMO1* promoter, indicating that *AsFMO1* is likely a downstream target regulated by AsWRKY9.

AsWRKY9 enhances AsFMO1 activity

Dual-luciferase assays were performed to validated the effects of AsWRKY9 on the promoter activity of *AsFMO1*. As shown in Fig. 5, the co-transformation of AsFMO1pro:LUC and 35Spro:AsWRKY9 had significantly higher luciferase activities than the co-transformation of AsFMO1pro:LUC and 35Spro (as control). These results suggested that AsWRKY9 positively regulates the promoter activity of *AsFMO1*. The OD_{340} values of NADPH at different concentrations were measured to construct a standard curve (Fig. 6A). By calculating the consumption of NADPH, the enzyme activity of AsFMO1 was evaluated. Enzyme activity assays further demonstrated that the enzyme activity in the callus of the pHB-vector group was 17.15 U, while in the pHB-AsWRKY9 group, it increased to 19.73 U, indicating that the enzyme activity in AsWRKY9-OE was higher than the control (Fig. 6B).

Overexpression of AsWRKY9 increased alliin content

To validate the function of AsWRKY9 in the alliin biosynthesis process, we introduced pHB-AsWRKY9 and a control plasmid pHB-vector into garlic callus (Fig. 6C). Alliin content analysis conducted across three independent transgenic lines showed that pHB-AsWRKY9 callus increased alliin levels to 0.019 ± 0.001 mg/L, 1.9-fold higher than controls.

Discussion

Alliin, a sulfur-containing amino acid unique to garlic, directly influences the flavor characteristics and medicinal properties of garlic, thus serving as a key indicator for assessing its quality. It plays a crucial role in garlic growth, development, and stress resistance. Yoshimoto et al. identified the mature leaves as the primary site for alliin biosynthesis, with alliin being transported to new shoots after the formation of new leaves, where it helps protect the young shoots from microbial and herbivorous attacks [14]. Studies have shown that when garlic cells are disrupted, alliin is converted into allicin by alliinase, which has significant antibacterial and anti-inflammatory effects and can prevent cancer, treat cardiovascular diseases, and enhance immunity. As the sole precursor of allicin, the molecular regulatory mechanism of alliin biosynthesis remains largely unknown. WRKY TFs play a crucial role in regulating the biosynthesis of plant secondary metabolites, thereby enhancing plant self-defense

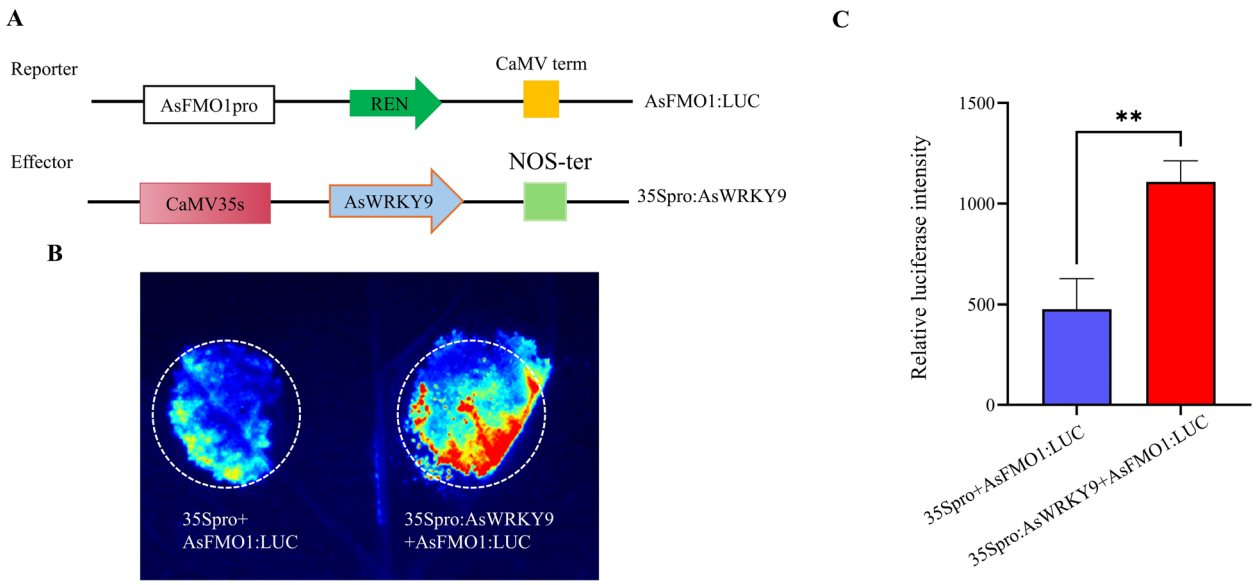

Fig. 5 Transcriptional activation ability of AsWRKY9. **A** Schematic view of the plasmid combinations of LUC reporters and effector. The promoter fragments of *AsFMO1* were cloned into the pGreenII 0800-LUC vector to generate the reporter constructs. The effector was generated by recombining the AsWRKY9 gene into the pHB-GFP vector. LUC, firefly luciferase; REN, Renilla luciferase. **B** Effects of AsWRKY9 on the promoter activity of *AsFMO1*as demonstrated by luciferase reporter assay. **C** Quantitative analysis of luminescence intensity. Three biological replicates were performed. The *p*-values were evaluated using Student's *t*-test. Stars indicate the level of significance, *$0.01 < p < 0.05$, and **$p < 0.01$

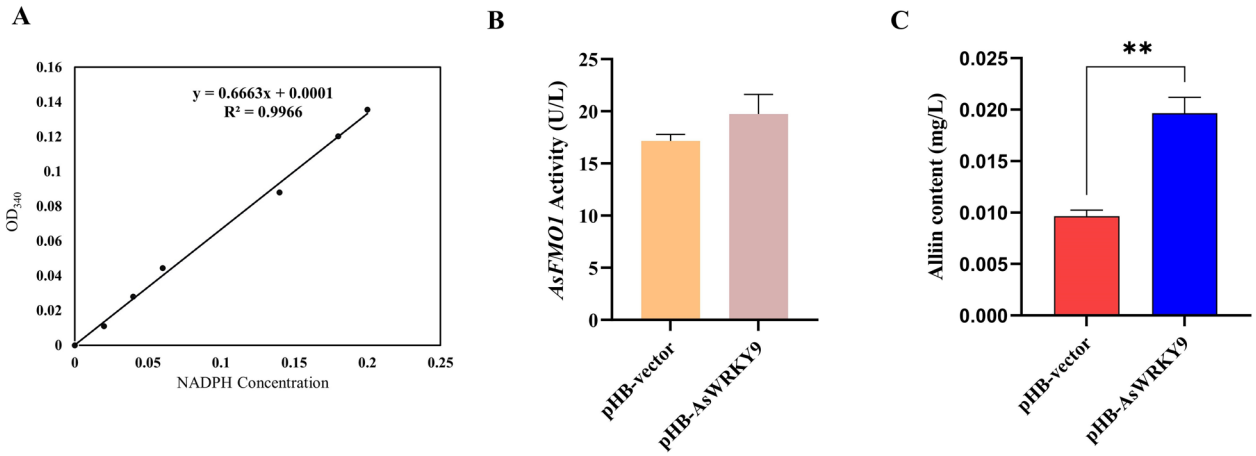

Fig. 6 AsWRKY9 boosts *AsFMO1* activity and alliin production in *Allium sativum* L. **A** NADPH concentration standard curve for measuring AsFMO1 enzyme activity, with NADPH concentration on the *X*-axis and OD_{340} values on the *Y*-axis. **B** Comparison of *AsFMO1* enzyme activity between pHB-AsWRKY9 overexpression and pHB-vector control groups. **C** The amino acid reagent organizer quantified the contents of alliin in the control and AsWRKY9. The *p*-values were evaluated using Student's *t*-test. Stars indicate the level of significance, $^{**}p < 0.01$, and $^{*}0.01 < p < 0.05$

capabilities. Yin et al. demonstrated that VqWRKY31 could enhance the resistance of grapevines by activating salicylic acid defense signaling to promote the biosynthesis of flavonoid derivatives [31]. Chen et al. found that AaWRKY17 binds to the *ADS* gene to promote the accumulation of artemisinin, with overexpressing AaWRKY17 increases the tolerance of *Artemisia annua* to *Pseudomonas syringae* [32]. Considering the bioactivity and biosynthetic conditions of alliin, we believe that the garlic WRKY family is a major regulator of alliin biosynthesis.

In our research, we initially identified 21 WRKY family members named AsWRKY1-21 using Yang et al. [30] reference-free transcriptome (due to the lack of a garlic genome). Based on the main biosynthesis sites of alliin, we subjected mature garlic leaves to mechanical injury at different times (3 h, 6 h, 12 h) and analyzed the expression levels of these 21 genes at three time points using qRT-PCR (Fig. 1A), with untreated leaves as controls. Compared to the control, the expression levels of *AsWRKY3*, *AsWRKY4*, *AsWRKY9*, *AsWRKY19*, and *AsWRKY21* were significantly upregulated at 3 h, indicating that these 5 genes could rapidly respond to external stimuli in a short term, while other genes took longer to be expressed. Interestingly, at 6 h only *AsWRKY9* exhibited a significant upregulation, suggesting that *AsWRKY9* might have transitioned from an early response to a mid-term synthetic defense mechanism. At 12 h, the expression levels of *AsWRKY3*, *AsWRKY4*, *AsWRKY9*, and *AsWRKY19* were significantly upregulated, possibly regulated by the feedback mechanism of alliin accumulation or changes in cellular status, ultimately leading to the reactivation of *AsWRKY3*, *AsWRKY4*, and *AsWRKY19* genes. Additionally, *AsWRKY9* showed significant upregulation at different treatment periods, indicating that *AsWRKY9* might play a key role in the regulatory mechanism of alliin biosynthesis. Based on these results, we preliminarily identified 5 genes (*AsWRKY3*, *AsWRKY4*, *AsWRKY9*, *AsWRKY19*, and *AsWRKY21*) and further analyzed their protein structures. Compared to AsWRKY3, AsWRKY4, and AsWRKY21, AsWRKY19 contains a WRKY conserved domain and a Plant-zn-clust domain (Fig. 1B), which may play a key role in regulating the production of plant secondary metabolites and resistance [33]. Genetic transformation is fundamental for studying gene function, and the preparation of callus tissue is crucial for genetic transformation [34]. Although there are studies on the preparation of garlic callus tissue, the induction rate of callus tissue varies greatly among varieties. Here, we propose an efficient callus induction system suitable for "PiZi" garlic, using garlic bulb scales as explants, MS as the basic culture medium, and a hormonal ratio of 1.5 mg/L 2,4-D + 0.5 mg/L NAA to induce substantial callus tissue formation in "PiZi" garlic bulb scales. The transformation efficiency in the established *Agrobacterium*-mediated garlic genetic transformation system is generally low. Based on Eady et al. [35] garlic genetic transformation, we optimized the genetic transformation system, mainly by selecting *Agrobacterium* (LBA4404 adjusted to GV3101), fixing the $OD_{550} = 0.6$ for the best effect, adjusting the infection time (from 5 to 30 min), and extending the co-cultivation time (from 6 to 7 days). Subsequently, calluses overexpressing pHB-GFP (control), AsWRKY3, AsWRKY4, AsWRKY9, AsWRKY19, and AsWRKY21 were obtained using *Agrobacterium infection*. Currently, the alliin biosynthesis pathway is unclear, but γ-glutamyl transpeptidase

genes (*AsGGT1*, *AsGGT2*, and *AsGGT3*) and a flavin-containing monooxygenase gene (*AsFMO1*) have been confirmed to catalyze the last two steps of this pathway. The expression levels of the *AsGGT1*, *AsGGT2*, *AsGGT3*, and *AsFMO1* genes in overexpressed and control calluses were analyzed using qRT-PCR. It was found that the expression level of the *AsFMO1* gene in AsWRKY9-OE was significantly higher compared to the control. Therefore, we speculate that AsWRKY9 may promote the biosynthesis of alliin by regulating the activation of *AsFMO1*. Summarizing the above results, we finally selected AsWRKY9 as a candidate gene in the alliin biosynthesis pathway. To verify our hypothesis, further studies on AsWRKY9 were conducted. Bioinformatics analysis showed that the AsWRKY9 protein consists of 267 amino acids, with a MW of 29.49 kDa and an pI of 9.79, indicating strong alkalinity. Subcellular localization confirmed that AsWRKY9 is located in the nucleus. Phylogenetic analysis revealed that AsWRKY9 is most closely related to NtWRKYY2 and NtWRKYJ2 (Fig. 2B). However, there are no reports on the functions of NtWRKYY2 and NtWRKYJ2 to date. Through comparison with the *Arabidopsis* database (https://www.arabidopsis.org/), we found that AsWRKY9 has high homology with AtWRKY11 (AT4G31552.2), belonging to the Group II-d subfamily of the WRKY family. Ali et al. verified that AtWRKY11 could coordinate the jasmonic acid (JA) and salicylic acid (SA) signaling pathways against *Bacillus*, enhancing drought tolerance in *Arabidopsis* and promoting seed germination and root growth [36]. Robatzek et al. found that after mechanical damage, the expression level of AtWRKY11 was upregulated [37]. This is similar to our speculation that AsWRKY9 enhances garlic resistance by increasing the biosynthesis of alliin after stress (mechanical injury treatment). Additionally, we examined the expression of AsWRKY9 in different garlic tissues (root, stalk, leaves, bulb) and found the highest expression in leaves, consistent with the main biosynthesis site of alliin being in leaves. Based on the results from Fig. 1C, we amplified the *AsFMO1* promoter sequence using chromosome walking due to the absence of the garlic genome at the time. The promoter was divided into three segments (AsFMO1-F1, AsFMO1-F2, AsFMO1-F3), and through YIH, we determined that AsWRKY9 bind to the W-box site of AsFMO1-F3. Based on the enzyme activity of the crude enzyme solution from transgenic calluses measured at 340 nm, compared to pHB-vector overexpressed calluses, the enzyme activity of *AsFMO1* was significantly upregulated in AsWRKY9 transgenic calluses. Additionally, LUC also verified that AsWRKY9 enhanced the expression level of *AsFMO1* enzyme activity. EMSA and ChIp-qPCR also confirmed that AsWRKY9 can directly bind to the *AsFMO1* promoter. Finally, amino acid analysis was used to measure the alliin content in AsWRKY9 overexpressed calluses. Compared to the control, the alliin content in overexpressed AsWRKY9 increased by 1.9-fold. Based on these results, a functional model for the role of AsWRKY9 in alliin biosynthetic regulation in *Allium sativum* is proposed (Fig. 7). In summary, we have ultimately determined that AsWRKY9 can directly bind to the *AsFMO1* promoter and activate its

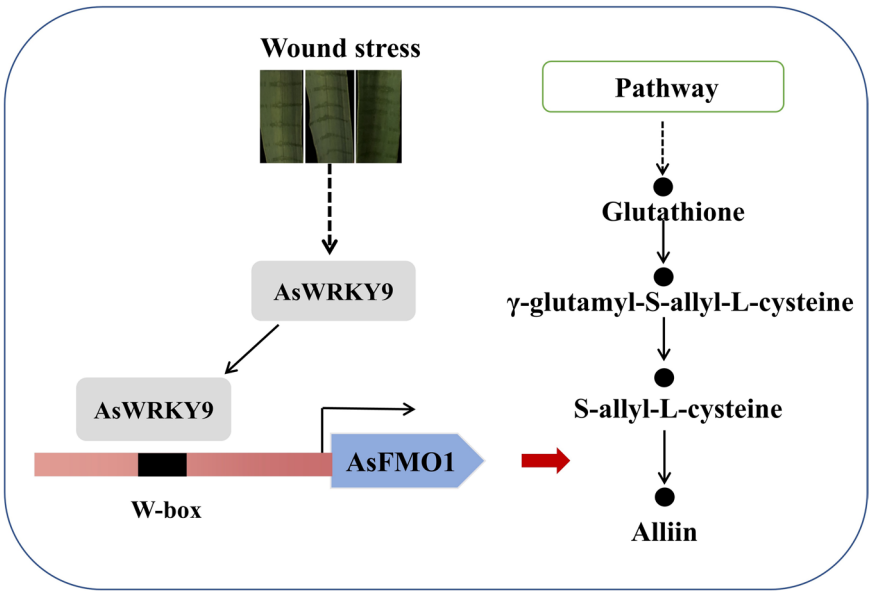

Fig. 7 A model for the role of AsWRKY9 in the alliin biosynthesis. W-box, WRKY recognition element

expression, thereby positively regulating the biosynthesis of alliin.

Conclusions

We identified a WRKY transcription factor gene, AsWRKY9, which showed significantly upregulated expression under clamping stress. AsWRKY9 is localized in the nucleus and contains both plant-zn-clust and WRKY domains. The expression of *AsFMO1* was markedly increased in callus overexpressing AsWRKY9. Further results revealed that AsWRKY9 binds to the W-box in the promoter region of *AsFMO1*, and by enhancing the activity of *AsFMO1*, it increases the alliin content in garlic callus, participating in the biosynthesis of alliin in garlic. In summary, our findings provide new insights into the mechanisms regulating the biosynthetic pathway of alliin in garlic.

Methods

Plant materials and treatment

The garlic cultivar "PiZi" used in this study were obtained from the Sanbao garlic planting base in Xuzhou (Jiangsu, China). These garlic cultivars were grown in pots containing soil in a greenhouse under short-day conditions (8 h light/16 h dark, 25 °C/18 °C, day/night) with a relative humidity of 65%. Leaves, stalks, roots, and bulbs were collected from two-mount old garlic seedling for gene expression analysis. Tissue specimens were collected from the third true leaves of garlic, grown under identical conditions. The leaves were gently pinched with tweezers to cause slight damage, and the treated area was collected after 3, 6, and 12 h. All samples were immediately frozen in liquid nitrogen and stored at − 80 °C until RNA extraction. The tobacco used in this study were grown in a greenhouse under normal-day conditions (12 h light/12 h dark, 22 °C, and 65% relative humidity). Callus were cultured at 22 °C in the dark and subcultured at 3-week intervals on the above solid medium.

Callus tissue culture preparation

To initiate garlic callus tissue culture, "PiZi" garlic bulb scales were first washed with water for 30 min, followed by immersion in 75% ethanol for 60 s, and then rinsed 5 times with water, each rinse lasting 1 min. Subsequently, the scales were soaked in 0.1% mercuric chloride solution for 15 min and rinsed 7 times with sterile water, each rinse also lasting 1 min. The sterilized garlic scales were cut into 1 mm pieces and inoculated onto MS medium with varying hormonal concentrations. The concentrations of 2,4-D were varied across 6 gradients (0.5, 1.0, 1.5, 2.0, 2.5, 3.0 mg/L) and NAA across 4 gradients (0.1, 0.5, 0.9, 1.3 mg/L), as detailed in the Additional file 1: Table. S1, with 15 scale tissues used per gradient. The cultures were incubated at 25 °C with 65% humidity under a light cycle of 16 h light/8 h dark for 30 days to identify the optimal medium for inducing callus in "PiZi" garlic scales.

Activation and transformation of target bacterial strain

The plasmids pHB-AsWRKY9-GFP and pHB-GFP (control) were transformed into *Agrobacterium tumefaciens* strain GV3101. Five microliters of bacterial suspension was added to 5 mL of LB medium supplemented with 5 μL of 50 mg/mL kanamycin and 5 μL of 50 mg/mL rifampicin and incubated overnight at 28 °C with shaking at 200 r/min. The next day, 2 mL of the overnight culture was transferred to 50 mL of LB medium containing 50 μL of 50 mg/mL kanamycin and 50 μL of 50 mg/mL rifampicin and incubated again overnight at 28 °C with shaking at 200 r/min. On the following day, an equal volume of LB medium with the same antibiotics concentrations was added, and the culture was shaken at 28 °C at 200 r/min for 4 h. The bacterial suspension was then centrifuged at 4 °C at 4000 r/min for 5 min, the supernatant was discarded, and the bacterial pellet was obtained. The pellet was resuspended in MS liquid medium, and when the $OD_{550}=0.6$, acetosyringone was added to a final concentration of 0.1 μM. Subsequently, 100 pieces of fresh garlic callus tissues were prepared 2 h in advance by grinding into fine particles and washed with sterile water until clear. The callus particles were suspended in 20 mL of MS liquid medium and gently shaken at 100 r/min at 28 °C to serve as the genetic transformation receptors. The calluses were immersed in the bacterial suspension for 30 min, after which they were rinsed three times with distilled water, dried on sterile filter paper, and transferred to MS medium containing 1.5 mg/L 2,4-D, 0.5 mg/L NAA and 200 mg/L cefotaxime for 7 days. Subsequently, the callus tissues were transferred to MS medium supplemented with 1.5 mg/L 2,4-D, 0.5 mg/L NAA, 10 mg/L hygromycin, and 200 mg/L cefotaxime for selection, and the transformation efficiency was assessed after 2–3 weeks.

Isolation and sequence analysis of AsWRKY9

RNA isolation was performed by the EASYspin plant RNA extraction kit (Aidlab Bio., China) according to the instructions. The RNA quality and quantity were determined using the NanoDrop2000c spectrophotometer (Thermo Fisher Scientific, USA), and RNA integrity was identified by electrophoresis on 1.0% agarose gels. cDNA was synthesized from 1 μg total RNA using the HiScript II QRT SuperMix for qPCR kit with gDNase (Vazyme, China) according to the manufacture protocols. Total

RNA was extracted from the leaves of "PiZi" garlic using the Plant RNA Extraction Kit (Aidlab, Beijing, China). Based on our transcriptome data [30], the AsWRKY9 F/R primer (Additional file 3: Table. S2) pairs were designed and used for cloning AsWRKY9 coding sequence from the cDNA of garlic. Then, the open reading frame (ORF) of AsWRKY9 was cloned into a pHB-GFP vector to create the 35S:GFP-AsWRKY9. The molecular weight and amino acid composition of AsWRKY9 were computed using the online website ExPASy ProtParam (https://web.expasy.org/protparam/). A BLAST search (https://www.ncbi.nlm.nih.gov/) was used for a homology search from the SWISS-PROT protein database. A phylogenetic tree was constructed using the MEGA 11 with the Neighbor-Joining algorithm, and the reliability of the branching pattern was tested with 1000 bootstrap repetitions. The online tool NCBI CD-Search was used to predict conserved domains in the encoded proteins (https://www.ncbi.nlm.nih.gov/Structure/bwrpsb/bwrpsb.cgi).

Quantitative real-time PCR

To determine the expression levels of AsWRKY9 in different tissues or treatments, qRT-PCR analysis was performed using the ABI StepOne Plus Real-time PCR systems (Thermol fisher, USA). One microliter of synthesized cDNA (diluted 1:5) was used as template for qRT-PCR. The *AsGAPDH* was selected as a reference gene (Additional file 3: Table. S2). Amplification cycles consisted of 30 s at 95 °C, followed by 40 cycles at 95 °C for 15 s and 60 °C for 30 s. Each measurement was performed using three biological replicates. The data was analyzed using the $2^{-\Delta\Delta CT}$ method.

Construction of overexpression vectors

The coding region of AsWRKY9 was derived from our previous transcriptome datasets of garlic. Specific primers were designed to amplify AsWRKY9 DNA segment from the cDNA of garlic using the following PCR parameters: initial denaturation at 94 °C for 90 s, 30 cycles of denaturation at 94 °C for 20 s, annealing at 55 °C for 20 s, extension at 72 °C for 90 s, and a final extension at 72 °C for 5 min. The PCR products were subcloned into pHB-GFP vector with *Hind* III restriction sites to form 35S:GFP-AsWRKY9.

Subcellular localization analysis

Transient expression in tobacco leaves was carried out as described in the literature [38]. To determine the subcellular localization of AsWRKY9, its full-length open reading frame (ORF) was constructed into the pCAMBIA1300-35S-GFP. The constructed fusion vector, containing green fluorescent protein (GFP), along with a nuclear marker, NLS-mCherry (red fluorescent protein), was transiently expressed in 4-week-old *N. benthamiana* leaves using the *Agrobacterium tumefaciens* GV3101 strain. The fluorescence signal was observed under a confocal laser scanning microscope (Leica SP8, Leica, Germany).

Cis-elements analysis of promoter sequences

Genome DNA was extracted using the Plant Genomic DNA extraction Kit (Aidlab Biotech, China) and used as a template. The specific primers for *AsFMO1* promoters were designed based on previous literature report [15], and the CDS region of *AsFMO1* was amplified using the genome walking technique. The primers used are listed in Additional file 3: Table. S2. Then, the online database PlantCARE (https://bioinformatics.psb.ugent.be/webtools/plantcare/html/) was used to identify the *cis*-acting elements of promoters.

Chromatin Immunoprecipitation PCR

ChIP was performed with the transgenic garlic callus harboring 35S:GFP-AsWRKY9 using the method reported in the literature [39]. The ChIP DNA products were analyzed by qRT-PCR using primers designed to amplify DNA fragments in the promoter regions of *AsFMO1* genes. The primer sequences for W-box were used for *AsFMO1* promoters respectively, and the primer sequences *AsFMO1* CDS served as an internal control (Additional file 3: Table. S2). These experiments were repeated more than three times.

Yeast one-hybrid assays

To confirm the interaction between AsWRKY9 and the promoter of *AsFMO1*, Y1H assays were performed using the blue-white selection. The full-length cDNA of AsWRKY9 was cloned into the *EcoR* I sites of the pB42AD activation vector to form pB42AD-AsWRKY9. The promoter fragment containing the putative W-box of *AsFMO1* promoter was amplified from the genome DNA of garlic with primers in Additional file 3: Table. S2. This fragment was then divided into three parts, and these fragments were cloned into the *Xho* I sites of the p178 vector to form p178-AsFMO1-F1/F2/F3, p178-mAsFMO1-F3 using ClonExpress II One step Clonging Kit (Vazyme, China). Then, the vectors were co-transformed into the yeast strain EGY48Gold using LiAc conversion protocols. Transformed yeast cells were dropped onto a selective medium containing synthetic dextrose (SD) without Ura and Trp (SD/-Trp/-Ura) and then screening for blue and white spots.

Electrophoretic mobility shift assays

AsWRKY9 CDS segment was subcloned into pGEX-4 T-1 vector to form GST-AsWRKY9 in which GST-tag was

fused into the N-terminal of the AsWRKY9. The resulting plasmid was transformed into *Escherichia coli* Rosetta (DE3). The 3′-end biotin W-box biotin probe corresponding to the W-box site was prepared (Sangon Bio, China) (Additional file 3: Table. S2). The W-box biotin was without biotin label and seted as competitor probe. The EMSA were performed using LightShift Chemiluminescent EMSA Kit (Thermo Scientific, USA) according to the manufacturer's instructions.

Dual-luciferase reporter assays

To further investigate the regulation of *AsFMO1* expression by AsWRKY9 protein, LUC reporter assays were performed. For transcriptional activity analysis, the coding region of AsWRKY9 was cloned into the pHB-GFP vector with *Hind* III under the control of the 35S promoter as effector (35Spro::AsWRKY9). The promoter sequence of *AsFMO1* was inserted into a pGreenII 0800-Luc vector and then co-transformed with 35Spro::AsWRKY9 or free pHB vector (35Spro, set as a negative control) into the tobacco leaves using an Agrobacterium-mediated method as described previously. After being cultivated in darkness for 6 h and under long-day conditions (16 h/8 h, day/night) for 36 h, the transformed leaves were sprayed with D-luciferin sodium salt (Solarbio, Beijing, China) and then were examined by using a Tanon 5200 multi-imaging apparatus (Tanon, Shanghai, China). Each assay was performed with three biological replicates. The sequences of primers were listed in Additional file 3: Table. S2.

Enzyme activity determination

To evaluate the enzyme activity of FMO using the consumption of NADPH, prepare a standard curve by measuring the OD_{340} values at NADPH concentrations of 0.02, 0.04, 0.06, 0.14, 0.18, and 0.20 mM. Fresh garlic callus tissue was collected, immediately frozen in liquid nitrogen, and ground to a fine powder. The ground tissue was then suspended in chilled extraction buffer and gently mixed. The suspension was then centrifuged at high speed at 4 °C to remove insoluble cell debris and impurities, and the supernatant was collected as the crude extract. The enzyme activity reaction components include the following: 50 mM Tris–HCl (pH=7.8), 500 μM NADPH, 1 mM DTT, and 0.1 mM EDTA. The OD_{340} value changes over 5 min were recorded using a multifunctional microplate reader, and the enzyme activity was calculated based on these absorbance changes. Under specific conditions, the amount of enzyme that consumes 1 μM of NADPH per minute is defined as one enzyme activity unit. The calculation formula is as follows:

$$U = \frac{\Delta c}{\Delta t} \times V$$

Δc:change in substrate concentration; Δt: reaction time; V: total volume of the reaction system.

Determination and analysis of alliin content

Garlic callus was collected, rapidly frozen in liquid nitrogen, and finely ground to prevent alliin degradation during processing. The powdered garlic was then mixed thoroughly with 4% sulfosalicylic acid (contains protease inhibitor cocktail), which helps protect alliin from oxidation. Then stored at 25 °C for 30 min. Centrifugation at 12,000 r/min for 20 min was then performed, and the content of alliin in the supernatant was determined by S-4330D amino acid analyzer. The alliin content is calculated using an automated process by the amino acid analyzer, which considers the standard concentrations, the peak areas from chromatographic analysis, the volumes of the samples introduced, and the dilution factors applied. This approach ensures precise quantification of the alliin mass fraction in the sample. To ensure the accuracy of the data, at least three replicates were obtained per tissue sample. Values represent the mean ± standard error.

Abbreviations

TF	Transcription factor
Y1H	Using yeast one-hybrid
ChIP	Chromatin immunoprecipitation
LUC	Dual-luciferase
EMSA	Electrophoretic mobility shift assay
AsFMO1	S-allyl-L-cysteine S-oxygenase
MW	Molecular weight
pI	Isoelectric point
JA	Jasmonic acid
SA	Salicylic acid

Supplementary Information

The online version contains supplementary material available at https://doi.org/10.1186/s12915-025-02116-y.

Additional file 1: Table S1. Callus induction rate and genetic conversion rate.

Additional file 2: Table S2. Primers used in this study.

Additional file 3: Figure S1. AsWRKY9 protein sequence compared with the Arabidopsis database was modified.

Additional file 4: Figure S2. Original gel image of the EMSA experiment.

Acknowledgements

We would like to express our sincere gratitude to all members of the Key Laboratory of Biotechnology for Medicinal Plants, Jiangsu Province, for their valuable contributions and support.

Authors' contributions

The research was designed by XY, JJ, JW conducted the experiments with the assistance of ML, JL, CL, QZ, CX, YS, CY, MZ and LZ. XM and YY from Jiangsu Nuen Crop Science Co., Ltd. also conducted the partial experiments. The paper was written by JW with assistance from ML. XY and JJ supervised the completion of the experiments. All authors contributed to the article and approved the submitted version. All authors read and approved the final manuscript.

Funding
This work were supported by the scientific and technological transformative project of Xuzhou (KC22438), the Serving "343" industry development project of University in Xuzhou (GX2023017), the Jiangsu province graduate research and practice innovation program project (KYCX24_3026), the Jiangsu Normal University graduate research innovation program (2024XKT1484), the Jiangsu Jieqing Reserve Project of Jiangsu Normal University (HB2016016), and the Jiangsu provincial advantage discipline construction project (PAPD). All of authors have read and agreed to the publication. The authors thank the lab members for assistance.

Data availability
The transcriptome sequencing data of garlic in this study can be found in the ENA Short Read Archive (https://www.ebi.ac.uk/ena), with accession number PRJEB33852.

Declarations

Ethics approval and consent to participate
Not applicable.

Consent for publication
Not applicable.

Competing interests
The authors declare no competing interests.

Author details
[1]The Key Laboratory of Biotechnology for Medicinal Plant of Jiangsu Province, School of Life Science, Jiangsu Normal University, Xuzhou, Jiangsu 221116, China. [2]Jiangsu Nuen Crop Science Co., Ltd., Xuzhou, Jiangsu 221116, China.

Received: 23 June 2024 Accepted: 3 January 2025
Published online: 13 January 2025

References

1. Maaß HI, Klaas M. Infraspecific differentiation of garlic (Allium sativum L.) by isozyme and RAPD markers. Theor Appl Genet. 1995;91:89–97. https://doi.org/10.1007/BF00220863.
2. Yang PT, Yuan Y, Yan C, Jia Y, You Q, Da LL, Lou A, Lv BS, Zhang ZH, Liu Y. AlliumDB: a central portal for comparative and functional genomics in *Allium*. Hortic Res. 2023;11:uhad285. https://doi.org/10.1093/hr/uhad285.
3. Ohri D, Fritsch RM, Hanelt P. Evolution of genome size in *Allium* (Alliaceae). Pl Syst Evol. 1998;210:57–86. https://doi.org/10.1007/BF00984728.
4. Zhang YW, Li LL, Ma XH, Liu RT, Shi RM, Zhao DS, Li XX. Extraction, purification, structural features, modifications, bioactivities, structure-activity relationships, and applications of polysaccharides from garlic: a review. Int J Biol Macromol. 2024;265(Pt2): 131165. https://doi.org/10.1016/j.ijbiomac.2024.131165.
5. Agarwal KC. Therapeutic actions of garlic constituents. Med Res Rev. 1996;16:111–24. https://doi.org/10.1002/(SICI)1098-1128(199601)16:1%3c111::AID-MED4%3e3.0.CO;2-5.
6. Gupta A, Mainkar P, Mahajan V. Exploring the nutritional-nutraceutical composition and phytochemical potential of garlic agents in preclinical and clinical studies with a focus on drug likeness. J Herbal Medicine. 2024;46:2210–8033. https://doi.org/10.1016/j.hermed.2024.100911.
7. Macpherson LJ, Geierstanger BH, Viswanath V, Bandell M, Eid SR, Hwang S, Patapoutian A. The pungency of garlic: activation of TRPA1 and TRPV1 in response to allicin. Curr Biol. 2005;15(10):929–34. https://doi.org/10.1016/j.cub.2005.04.018.
8. Hu L, Zhao PC, Wei YB, Lei YD, Guo X, Deng XR, Zhang J. Preparation and characterization study of zein–sodium caseinate nanoparticle delivery systems loaded with allicin. Foods. 2024;13:3111. https://doi.org/10.3390/foods13193111.
9. Gong QM, Wang XM, Liu YS, Yuan HL, Ge ZF, Li YZ, Huang JH, Liu YF, Chen M, Xiao WJ, Liu RT, Shi RM, Wang LP. Potential hepatoprotective effects of allicin on carbon tetrachloride-induced acute liver injury in mice by inhibiting oxidative stress, inflammation, and apoptosis. Toxics. 2024;12:328. https://doi.org/10.3390/toxics12050328.
10. Bhuker S, Kaur A, Rajauria K, Tuli HS, Saini AK, Saini RV, Gupta M. Allicin: a promising modulator of apoptosis and survival signaling in cancer. Med Oncol. 2024;41:210. https://doi.org/10.1007/s12032-024-02459-6.
11. Talib WH, Baban MM, Azzam AO, Issa JJ, Ali AY, AlSuwais AK, Allala S, AL Kury LT. Allicin and cancer hallmarks. Article 1320. 2024;29:1320. https://doi.org/10.3390/molecules29061320.
12. Sleiman C, Daou RM, Al Hazzouri A, Hamdan Z, Ghadieh HE, Harbieh B, Romani M. Garlic and hypertension: efficacy, mechanism of action, and clinical implications. Nutrients. 2024;16: 2895. https://doi.org/10.3390/nu16172895.
13. Borlinghaus J, Albrecht F, Gruhlke MC, Nwachukwu ID, Slusarenko AJ. Allicin: chemistry and biological properties. Molecules. 2014;19:12591–618. https://doi.org/10.3390/molecules190812591.
14. Yoshimoto N, Saito K. S-Alk(en)ylcysteine sulfoxides in the genus Allium: proposed biosynthesis, chemical conversion, and bioactivities. J Exp Bot. 2019;70:4123–37. https://doi.org/10.1093/jxb/erz243.
15. Yoshimoto N, Onuma M, Mizuno S, Sugino Y, Nakabayashi R, Imai S, Tsuneyoshi T, Sumi S, Saito K. Identification of a flavin-containing S-oxygenating monooxygenase involved in alliin biosynthesis in garlic. Plant J. 2015;83:941–51. https://doi.org/10.1111/tpj.12954.
16. Suzuki T, Sugii M, Kakimoto T. New γ-glutamyl peptides in garlic. Chem Pharm Bull. 1961;9:77–8. https://doi.org/10.1248/cpb.9.77.
17. Suzuki T, Sugii M, Kakimoto T. Metabolic incorporation of L-valine-[14C] into S-(2-carboxypropyl) glutathione and S-(2-carboxypropyl) cysteine in garlic. Chem Pharm Bull (Tokyo). 1962;10:328–31. https://doi.org/10.1248/cpb.10.328.
18. Granroth B. Biosynthesis and decomposition of cysteine derivatives in onion and other Alliu specie. Helsingfors Suomalainen Tiedeakat Toimituksia Ser A Ii Chem. 1970. https://api.semanticscholar.org/CorpusID:90996924.
19. Lancaster JE, Shaw ML. γ-Glutamyl peptides in the biosynthesis of S-alk(en)yl-L-cysteine sulphoxides (flavour precursors) in *Allium*. Phytochemistry. 1989;28:455–60. https://doi.org/10.1016/0031-9422(89)80031-7.
20. Sun XD, Zhu SY, Li NY, Cheng Y, Zhao J, Qiao XG, Lu L, Liu SQ, Wang YZ, Liu C, Li BP, Guo W, Gao S, Yang ZM, Li F, Zeng Z, Tang Q, Pan YP, Guan MJ, Zhao J, Lu XM, Meng HW, Han ZL, Gao CS, Jiang WK, Zhao X, Tian SL, Su JG, Cheng ZH, Liu TM. A chromosome-level genome assembly of garlic (*Allium sativum*) provides insights into genome evolution and allicin biosynthesis. Mol Plant. 2020;13:1328–39. https://doi.org/10.1016/j.molp.2020.07.019.
21. Rao A, Luo C, Hogan PG. Transcription factors of the NFAT family: regulation and function. Annu Rev Immunol. 1997;15:707–47. https://doi.org/10.1146/annurev.immunol.15.1.707.
22. Eulgem T, Rushton PJ, Robatzek S, Somssich IE. The WRKY superfamily of plant transcription factors. Trends Plant Sci. 2000;5:199–206. https://doi.org/10.1016/s1360-1385(00)01600-9.
23. Xie T, Chen CJ, Li CH, Liu JR, Liu CY, He YH. Genome-wide investigation of WRKY gene family in pineapple: evolution and expression profiles during development and stress. BMC Genomics. 2018;19:490. https://doi.org/10.1186/s12864-018-4880-x.
24. Chen H, Lai ZB, Shi JW, Xiao Y, Chen ZX, Xu XP. Roles of *arabidopsis* WRKY18, WRKY40 and WRKY60 transcription factors in plant responses to abscisic acid and abiotic stress. BMC Plant Biol. 2010;10:281. https://doi.org/10.1186/1471-2229-10-281.
25. Qu J, Xiao P, Zhao ZQ, Wang YL, Zeng YK, Zeng X, Liu JH. Genome-wide identification, expression analysis of WRKY transcription factors in *Citrus ichangensis* and functional validation of CiWRKY31 in response to cold stress. BMC Plant Biol. 2024;24(1):617. https://doi.org/10.1186/s12870-024-05320-0.
26. Zhang GL, Sun YE, Ullah N, Kasote D, Zhu LY, Liu H, Xu L. Changes in secondary metabolites contents and stress responses in Salvia miltiorrhiza via ScWRKY35 overexpression: insights from a wild relative *Salvia castanea*. Plant Physiol Biochem. 2024;211: 108671. https://doi.org/10.1016/j.plaphy.2024.108671.
27. Xiao SH, Ming YQ, Hu Q, Ye ZX, Si H, Liu SM, Zhang XJ, Wang WR, Yu Y, Kong J, Klosterman SJ, Lindsey K, Zhang XL, Aierxi A, Zhu LF. GhWRKY41 forms a positive feedback regulation loop and increases cotton defence response against Verticillium dahliae by regulating phenylpropanoid

metabolism. Plant Biotechnol J. 2023;21:961–78. https://doi.org/10.1111/pbi.14008.
28. Tao H, Miao HY, Chen LL, Wang MY, Xia CC, Zeng W, Sun B, Zhang F, Zhang SQ, Li CY, Wang QM. WRKY33-mediated indolic glucosinolate metabolic pathway confers resistance against *Alternaria brassicicola* in *Arabidopsis* and *Brassica* crops. J Integr Plant Biol. 2022;64:1007–19. https://doi.org/10.1111/jipb.13245.
29. Yuan Y, Ren SY, Liu XF, Su LY, Wu Y, Zhang W, Li Y, Jiang YD, Wang HH, Fu R, Bouzayen M, Liu MC, Zhang Y. SlWRKY35 positively regulates carotenoid biosynthesis by activating the MEP pathway in tomato fruit. New Phytol. 2022;234:164–78. https://doi.org/10.1111/nph.17977.
30. Yang XQ, Su YR, Wu JY, Wan W, Chen HJ, Cao XY, Wang JJ, Zhang Z, Wang YZ, Ma DL, Loake GJ, Jiang JJ. Parallel analysis of global garlic gene expression and alliin content following leaf wounding. ENA. 2019. https://www.ebi.ac.uk/ena/browser/view/PRJEB33852?show=related-records.
31. Yin WC, Wang XH, Liu H, Wang Y, Nocker S, Tu MX, Fang JH, Guo JQ, Li Z, Wang XP. Overexpression of VqWRKY31 enhances powdery mildew resistance in grapevine by promoting salicylic acid signaling and specific metabolite synthesis. Hortic Res. 2022;9: uhab064. https://doi.org/10.1093/hr/uhab064.
32. Chen TT, Li YP, Xie LH, Hao XL, Liu H, Qin W, Wang C, Yan X, Wu-Zhang KY, Yao XH, Peng BW, Zhang YJ, Fu XQ, Li L, Tang KX. AaWRKY17, a positive regulator of artemisinin biosynthesis, is involved in resistance to *Pseudomonas syringae* in *Artemisia annua*. Hortic Res. 2021;8:217. https://doi.org/10.1038/s41438-021-00652-6.
33. Shen L, Xia X, Zhang LH, Yang SX, Yang X. SmWRKY11 acts as a positive regulator in eggplant response to salt stress. Plant Physiol Biochem. 2023;205: 108209. https://doi.org/10.1016/j.plaphy.2023.108209.
34. Ikeuchi M, Ogawa Y, Iwase A, Sugimoto K. Plant regeneration: cellular origins and molecular mechanisms. Development. 2016;143:1442–51. https://doi.org/10.1242/dev.134668.
35. Eady C, Davis S, Catanach A, Kenel F, Hunger S. Agrobacterium tumefaciens-mediated transformation of leek (*Allium porrum*) and garlic (*Allium sativum*). Plant Cell Rep. 2005;24:209–15. https://doi.org/10.1007/s00299-005-0926-z.
36. Ali MA, Azeem F, Nawaz MA, Acet T, Abbas A, Imran QM, Shah KH, Rehman HM, Chung G, Yang SH, Bohlmann H. Transcription factors WRKY11 and WRKY17 are involved in abiotic stress responses in *Arabidopsis*. J Plant Physiol. 2018;226:12–21. https://doi.org/10.1016/j.jplph.2018.04.007.
37. Robatzek S, Somssich. IE. A new member of the *Arabidopsis* WRKY transcription factor family, AtWRKY6, is associated with both senescence- and defence-related processes. Plant J. 2001;28(2):123–33. https://doi.org/10.1046/j.1365-313x.2001.01131.x.
38. Kato N, Pontier D, Lam E. Spectral profiling for the simultaneous observation of four distinct fluorescent proteins and detection of protein-protein interaction via fluorescence resonance energy transfer in tobacco leaf nuclei. Plant Physiol. 2002;129(3):931–42. https://doi.org/10.1104/pp.005496.
39. Meng LM, Xu MK, Wan W, Yu F, Li C, Wang J, Wei ZQ, Lv MJ, Cao XY, Li ZY, Jiang JH. Sucrose Signaling Regulates Anthocyanin Biosynthesis Through a MAPK Cascade in *Arabidopsis thaliana*. Genetics. 2018;210:607–19. https://doi.org/10.1534/genetics.118.301470.

Publisher's Note